

## Original Article



## OPEN ACCESS

**Received:** Aug 23, 2020

**Revised:** Oct 20, 2020

**Accepted:** Dec 21, 2020

### Address for Correspondence:

**Ankur Chaudhury, MD, M. Eng.**

Department of Internal Medicine, Drexel University College of Medicine, 245 N 15th Street, 6th floor, Philadelphia, PA 19102, USA.  
E-mail: Ankur.chaudhury18@gmail.com

**Andrew Kohut, MD, MPH**


Department of Cardiology, Penn Heart and Vascular Center Washington Square, 800 Walnut St. 9th Floor, University of Pennsylvania Health System, Philadelphia, PA 19104, USA.  
E-mail: Andrew.kohut@penmedicine.upenn.edu


Copyright © 2021 Korean Society of


Echocardiography


This is an Open Access article distributed under the terms of the Creative Commons Attribution Non-Commercial License (<https://creativecommons.org/licenses/by-nc/4.0/>) which permits unrestricted non-commercial use, distribution, and reproduction in any medium, provided the original work is properly cited.

### ORCID iDs

Ankur Chaudhury   
<https://orcid.org/0000-0001-6759-9810>

Devasena Ponnalagu   
<https://orcid.org/0000-0003-2731-9778>

Harpreet Singh   
<https://orcid.org/0000-0002-6135-1897>

Andrew Kohut   
<https://orcid.org/0000-0002-9038-3599>

# Use of Speckle Tracking Echocardiography to Detect Induced Regional Strain Changes in the Murine Myocardium by Acoustic Radiation Force

**Ankur Chaudhury , MD, M. Eng.<sup>1</sup>, Austin Wanek, BS<sup>2</sup>, Devasena Ponnalagu , PhD<sup>3</sup>, Harpreet Singh , PhD<sup>3</sup>, and Andrew Kohut , MD, MPH<sup>4</sup>**

<sup>1</sup>Department of Internal Medicine, Drexel University College of Medicine, Philadelphia, PA, USA

<sup>2</sup>Department of Biomedical Engineering, University of Cincinnati, Cincinnati, OH, USA

<sup>3</sup>Department of Physiology and Cell Biology, Davis Heart and Lung Research Institute, The Ohio State University Wexner Medical Center, Columbus, OH, USA

<sup>4</sup>Department of Cardiology, University of Pennsylvania Health System, Philadelphia, PA, USA

## ABSTRACT

**BACKGROUND:** It is difficult to simulate the abnormal myocardial strain patterns caused by ischemic coronary artery disease (CAD) which are a precursor to heart failure (HF) within an animal model. Simulation of these strain changes could contribute to better understanding of the early formative stages of HF. This is especially important in investigating the poorly understood pathogenesis of heart failure with preserved ejection fraction (HFpEF). Here, we discuss delivery of high intensity focused ultrasound (HIFU) in a murine model to alter left ventricular (LV) regional longitudinal strain (RLS), and use of speckle tracking echocardiography to detect these changes.

**METHODS:** HIFU pulses (pressure amplitude 1.7 MPa) were generated by amplifying a sinusoidal waveform from a function generator into a piezoelectric transducer. These pulses were then directed extracorporeally towards the anterior LV surface of C57Bl6 mice during three time periods (early, mid, and late diastole). Speckle tracking echocardiography was then used to quantify changes in RLS within six segments of the LV.

**RESULTS:** We observed an increase in LV RLS with acoustic augmentation during all three time periods. This augmentation was most prominent near the anterior apical region in early diastole and near the posterior basilar region during late diastole.

**CONCLUSIONS:** Our findings demonstrate the application of HIFU to non-invasively induce changes in RLS within a murine model. Our results also reflect the capability of speckle tracking echocardiography to analyze and quantify these changes. These findings represent the first demonstration of ultrasound-induced augmentation in LV RLS within a small animal model.

**Keywords:** Echocardiography; Strains; High-intensity focused ultrasound therapy

## INTRODUCTION

The divergent mechanisms which lead to either heart failure with reduced ejection fraction (HFrEF) or heart failure with preserved ejection fraction (HFpEF) in patients with ischemic

**Funding**

This work is supported by a grant from the W. W. Smith Charitable Trust (AK and HS), American Heart Association Grant in Aid (16GRNT29430000, HS), National Institute of Health (R01-HL133050, HS) and Commonwealth University Research Enhancement Grants (AK and HS).

**Conflict of Interest**

The authors have no financial conflicts of interest.

**Author Contributions**

Conceptualization: Kohut A; Data curation: Chaudhury A, Wanek A; Formal analysis: Chaudhury A, Singh H, Kohut A; Funding acquisition: Singh H; Investigation: Chaudhury A, Wanek A; Methodology: Chaudhury A, Ponnalagu D, Kohut A; Resources: Singh H; Supervision: Singh H, Kohut A; Visualization: Kohut A; Writing - original draft: Chaudhury A; Writing - review & editing: Chaudhury A, Singh H, Kohut A.

coronary artery disease (CAD) are complex and difficult to model. One common feature of these diseases, regardless of their etiology, are early strain changes within the cardiac myocardium.<sup>1-4)</sup> Measurement of abnormal cardiac strain changes has already been validated as a predictor of left ventricular (LV) remodeling early after myocardial infarction (MI). Regional changes in LV strain occur within days of MI, preceding the process of infarct progression and eccentric hypertrophy which take months to years to occur.<sup>1)</sup> However, within the continuum of ischemic heart disease, changes in myocardial strain patterns do not require the catastrophic plaque rupture which results in MI. Initial strain changes far precede these total occlusion events. In patients with CAD, transient stress-induced local ischemia results in intermittent, aberrant strain changes in corresponding regions of the myocardium. In fact, comparison of areas of abnormal regional longitudinal strain (RLS) using speckle tracking echocardiography (STE) correlate well to areas of ischemia as confirmed by coronary angiography (the gold standard).<sup>5)</sup> Without clinical intervention, areas with pathological strain patterns are prone to LV remodeling which can eventually lead to heart failure (HF).<sup>6,7)</sup> Patients with CAD are therefore a population within which early detection of abnormal myocardial strain patterns would be a useful tool to predict risk of progression to HF, allowing for more timely clinical intervention.

An experimental animal model which can mimic the regional myocardial strain changes seen in patients with 'stuttering' or unstable angina who eventually develop HF would be an important tool to better understand the pathogenesis of the disease. However, creating such a model remains a challenge, as no convenient method exists which can mimic the transient, intermittent myocardial strain changes caused by changes in blood flow which occur early in the pathogenesis of HFrEF and HFpEF. Most currently validated small animal HF models study later stages of the disease. In addition the majority of these models induce HFrEF; far fewer models exist which are able to reliably provoke HFpEF.<sup>8)</sup> Many of the methods used to induce HFrEF in small animal models, such as transverse aortic constriction (TAC), coronary artery ligation, and aorto-caval shunt formation, present additional challenges. For instance, these methods involve surgical procedures, which are invasive, require a high level of technical skill, and are associated with risk of mortality from ventricular arrhythmias and heart block.<sup>9)</sup> Methods used to induce HFpEF in small animal models (such as the Dahl salt-sensitive rats, senescence accelerated prone [SAMP] mice, and streptozotocin [STZ] toxicity mediated models), are both time intensive and better suited to studying HFpEF once it is established rather than the early mechanistic changes of the disease.<sup>10)</sup> These HFpEF models also result in global myocardial changes which more closely mimic systemic causes of HFpEF (such as infiltrative disease), rather than the regional myocardial changes which occur in ischemic disease.

In this study, we demonstrate the feasibility of inducing transient regional myocardial strain changes using targeted extracorporeal high intensity focused ultrasound (HIFU) pulse delivery. HIFU is an application of acoustic radiation force (ARF), which is a term that describes the transfer of momentum an acoustic perturbation (such as an ultrasound wave) imparts as it passes through a nonlinear medium. ARF has been historically widely utilized within the field of medicine for applications ranging from cataract emulsification to renal stone lithotripsy.<sup>11,12)</sup> However, ARF can also be harnessed to deliver force in a tempered manner, exerting pressure on tissues without causing tissue destruction. In 2016, Marquet et al.,<sup>13)</sup> used HIFU pulses (1 MHz central frequency, with acoustic pressure 6 MPa over 50  $\mu$ s to 1 ms, and 4 MPa over 1 to 10 ms) to successfully perform continuous extracorporeal pacing in a swine model. In these experiments the Marquet team was able to use a HIFU

beam to precisely (focal width 1.8 mm) target different regions of myocardium within the atria and the ventricles, and elicit a consistent electromechanical stimulation response, without causing any cardiac tissue damage. We hypothesized that when HIFU is delivered at lower acoustic pressures (1.7 MPa) over a greater area (focal width 5 mm) compared to those used by Marquet et al<sup>13)</sup>, the imparted ARF would mechanically deform the myocardium without inducing a pacing focus. We used speckle tracking echocardiography to analyze and compare changes in strain with and without HIFU augmentation using regional longitudinal strain (RLS) as the variable of comparison. Speckle tracking echocardiography is a technique which uses tracking algorithms to follow the position of kernels (small regions within the myocardium each with a unique speckle pattern), frame-by-frame within an echocardiogram.<sup>14)</sup> This approach allows detection of subtle changes in cardiac physiology not attainable by traditional echocardiography. The ability to extracorporeally induce transient strain changes within the myocardium of a small animal model, and to measure these changes could serve as a powerful clinical tool to study the early pathogenesis of ischemia induced HFrEF and HFpEF.

## METHODS

### HIFU characteristics

The capabilities of the HIFU apparatus used in these experiments (see **Figure 1** for details regarding transducer setup) were first tested using a hydrophone (see **Table 1** for recorded pressure readings). These acoustic pressures are recorded after the ultrasound wave has traveled 7.7 cm from the transducer face through a gel filled plastic standoff. This length of the plastic standoff ensured that the ultrasound beam was in its focal zone (which is stable between 6-8 cm) when it exited the housing and struck the hydrophone. These recordings show that despite some expected pressure dampening within the tube (due to reflections and interference), a significant amount of pressure can still be generated by the beam after it exits the plastic standoff (310-864 kPa in the input voltage range tested). In prior literature, the upper estimate of Young's modulus of murine myocardium does not exceed 60 kPa.<sup>15)</sup> However, the actual acoustic pressure which must be delivered to the skin surface to induce

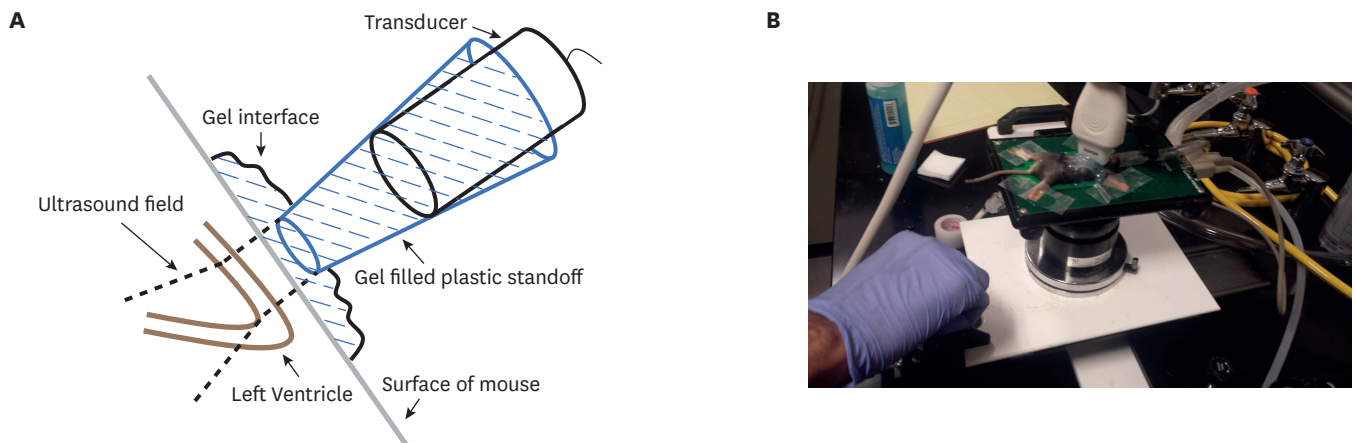


**Figure 1.** Transducer and positioning apparatus. (A) Schematic of ultrasound transducer housing and positioning apparatus. The transducer is housed within a 7.7 cm plastic standoff filled with coupling gel. The same coupling gel was spread in a thin layer on the parasternal surface of the mouse, ensuring uninterrupted transmission of ultrasound pulses. The ultrasound field is shown, with no divergence within the murine LV myocardium, which is within the axial focal zone of the transducer. (B) Mouse affixed to Physiologic Monitoring Unit with Vevo® imaging system probe in place. LV: left ventricular.

**Table 1.** Hydrophone pressure data

Function generator P-P output (mV)	Pressure at focal point 7.7 cm from transducer face (kPa)
100	310
150	405
200	524
250	601
300	691
400	804
450	864

myocardial strain changes is significantly higher than this theoretical value. This discrepancy is firstly because the beam must pass through skin, connective tissue, and bone, all of which would cause absorption and scattering. Secondly, Young's modulus is higher in *in vivo* myocardium since dynamic changes in myofilament configuration increases stiffness in systole, and potential energy stored during the contraction phase rebounds as elastic recoil during diastole.<sup>16)</sup> We therefore applied an input voltage sufficient to exert pressure an order of magnitude higher than that of the measured myocardial Young's modulus in literature. After fine tuning our input voltage based on careful evaluation of experimental results, we used an input voltage of 1 V (P-P) from the function generator for an acoustic pressure (extrapolated from hydrophone data in **Table 1**) of 1.7 MPa. We targeted the diastolic time period for these experiments because we suspected that the relaxed myocardium would yield to a greater extent under the impact of the ultrasound pulse as compared to stiffened myocardium during systole.

### Cardiac imaging

The experimental protocol was approved by the Drexel Institutional Animal Care and Use Committee. All experiments were conducted in accordance with the approved guidelines.<sup>17)</sup> A total of 10 female C57Bl6 mice (2-3 months old) of approximately the same size (~20-25 g) were selected (5 control and 5 experimental group). The animals' hair was removed using Nair hair removal lotion from their parasternal region to enable visualization of the heart during echocardiography. The mice were then affixed to a heated platform with electrocardiogram contact pads (THM-150; Indus Instruments, Houston, TX, USA). The mice underwent induction of anesthesia with 2.5% (*v/v*) isoflurane mixed with room air. The heart rate, respiratory rate, temperature, and a continuous EKG signal were monitored using the Vevo<sup>®</sup> 2100 linear imaging array (FUJIFILM VisualSonics, Inc., Toronto, Canada). Isoflurane concentrations were titrated (1-2%) targeting heart rates between 300 and 400 bpm to ensure stable sedation throughout the experiment. The MS400 probe mounted to the Vevo<sup>®</sup> 2100 system was used to capture real time images of the murine left ventricle (**Figure 1B**).

### Ultrasound pulse deliverance

To generate the ultrasound pulse, a signal generator (model No. 33220A; Agilent Technologies Inc., Santa Clara, CA, USA) was first used to generate an analog sine wave signal. Each signal consisted of a train of 8 sequential sinusoidal outputs of peak-to-peak voltage 1 V, frequency 2.5 MHz, and duration 5 ms. The total duration of the 8 sequential pulses was therefore 40 ms. This signal was outputted to a power amplifier (model No. 350L RF; Electronic Navigation Industries, Rochester, NY, USA) with gain of 50 dB. The amplified output was then fed into a flat-faced mono-element piezoelectric focused ultrasound transducer which generated an ultrasound pulse (**Figure 2**). The transducer had characteristics as follows: 11 mm aperture, center frequency 2.5 MHz, bandwidth 2.48-2.53 MHz, focal spot size 10 × 10 mm, stable over focal length 6-8 cm. To focus the ultrasound

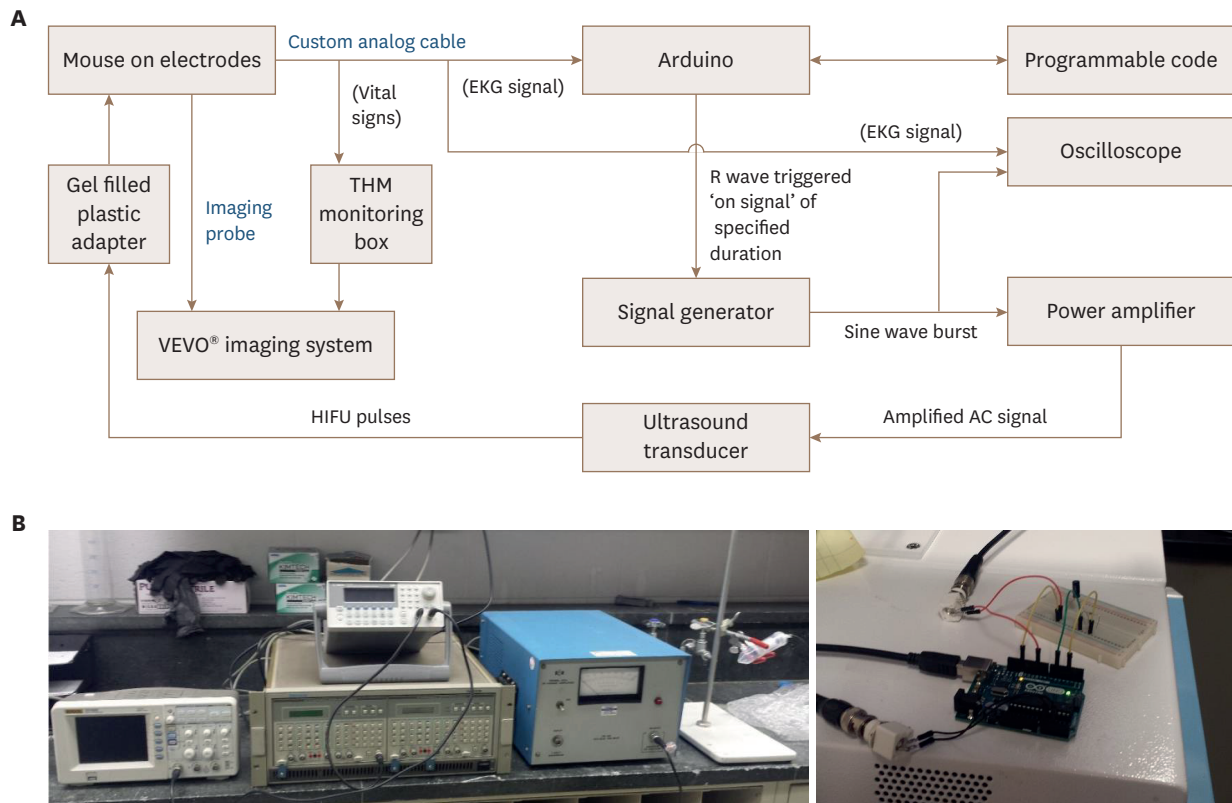


**Figure 2.** Experimental design and setup. (A) Schematic of the experimental setup. The murine EKG waveform interfaces with a microcontroller which recognizes an R wave and triggers the signal generator to release a sinusoidal signal after a specified onset. This signal is then amplified and transduced into an ultrasound pulse. Real time echocardiography is simultaneously performed, while the animal's vital signs were continuously monitored. (B) Image on bottom left shows the oscilloscope, signal generator, amplifier, and ultrasound transducer inside plastic standoff. The microcontroller circuit is pictured on bottom right. HIFU: high intensity focused ultrasound.

pulse, the transducer was placed in a columned standoff filled with coupling gel with a circular aperture of diameter 5 mm at the distal end. The surface of the ultrasound probe was positioned 7.7 cm from the left anterolateral chest wall. A microcontroller (Arduino Uno R3) and comparator circuit were used to synchronize the ultrasound pulses to 3 different periods within the cardiac cycle (early, mid, and late diastole). **Figure 2** provides a schematic of the overall setup. **Figure 1** illustrates the transducer setup relative to the surface of the mouse.

### Myocardial imaging

Ultrasound pulses were delivered to the mouse ventricle during three different times in the cardiac cycle (early, mid, and late diastole). A microcontroller was programmed to deliver ultrasound pulses every alternate heartbeat, so that myocardial strain during native beats (those without any acoustic pressure augmentation) could be compared to strain during pulsed beats (those with acoustic pressure augmentation). This method in theory would allow each animal to be used as its own control. The Vevo<sup>®</sup> 2100 system (FUJIFILM VisualSonics, Inc.) was used to obtain *in vivo* images of the murine left ventricle. We utilized B-mode imaging of the parasternal long axis view of the heart (**Figure 3**). Using the Vevo<sup>®</sup> Strain software package (FUJIFILM VisualSonics, Inc.), these images were uploaded for analysis. Both global strain and RLS were calculated using speckle tracking algorithms. The strain which was measured and reported was the maximal value attained over a single cardiac cycle. For beats with acoustic augmentation, this value inevitably occurred during the period when the ventricle was subjected to the ultrasound pulse.

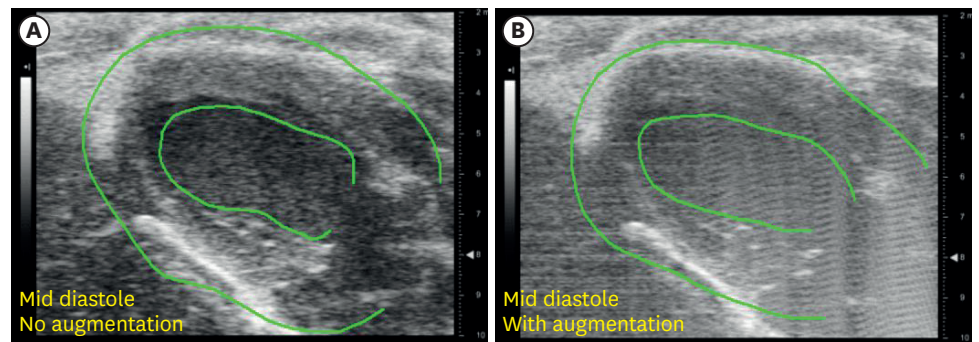


**Figure 3.** Echocardiography images with and without HIFU augmentation. (A) Representative echocardiography image of LV mid-diastole without acoustic augmentation. (B) Representative echocardiography image of LV mid-diastole during delivery of the HIFU pulse. As the HIFU pulse travels through the myocardium, ultrasound interference patterns are discernible, visible as a faint haze overlying the image. Despite this interference, the software is able to detect and track kernels across frames to provide us with usable strain data. HIFU: high intensity focused ultrasound, LV: left ventricular.

### Statistical analysis

The endocardial as well as the epicardial regions were separately traced and analyzed, and for each of these regions, 6 areas were analyzed separately (**Figure 4**), yielding peak RLS as the measured variable of comparison. In order to use the Vevo<sup>®</sup> Strain software to meaningfully calculate strain, the program had to first be able to identify the outer and inner boundaries of the myocardium and then accurately follow these traced boundaries throughout the entire cardiac cycle. Each calculated trace was visually inspected for correspondence with the actual movement of the myocardial wall. Any echocardiogram images which did not produce a satisfactory trace were manually excluded from data analysis. Within each time period, 5 control animals and 5 experimental animals were compared. However, for the above reason, the data could not be compared in a paired analysis. Statistical differences between the mean RLS of the two groups were therefore calculated using unpaired two-tailed two-sample Student's t-test assuming equal variance (Microsoft<sup>®</sup> Excel<sup>®</sup> 2016; Microsoft, Redmond, WA, USA). A p-value of less than 0.05 was considered significant.

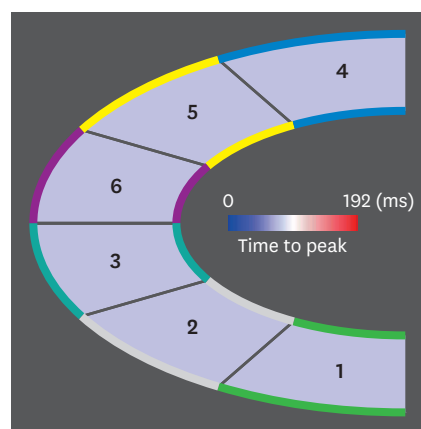


**Figure 4.** Left ventricular regions analyzed. 1 is posterior-base, 2 is posterior-mid, 3 is posterior-apex, 4 is anterior-base, 5 is anterior-mid, and 6 is anterior-apex.

## RESULTS

## Early diastolic ultrasound augmentation

The results of early diastolic delivery of HIFU pulses to the anterior LV surface are shown in **Figure 5**. To synchronize ultrasound delivery to the early diastolic period, an offset of 70 ms after recognition of an R wave peak was implemented. As noted previously, each ultrasound pulse consisted of a train of 8 sequential 5 ms sinusoidal outputs of peak-to-peak voltage 1 V and frequency 2.5 MHz, for a total ultrasound pulse delivery time of 40 ms. Every alternate beat received once such ultrasound pulse. As seen in **Figure 5**, the regions which experienced significant ( $p < 0.05$ ) increase in RLS with acoustic augmentation were the anterior-apex of the endocardium, as well as the anterior-mid region of the epicardium.

## Mid diastolic ultrasound augmentation

**Figure 6** shows the RLS measurements for mid-diastolic HIFU pulse delivery. To target the mid-diastolic period for delivery of the ultrasound pulse, we used an offset of 100 ms after the R-wave. The same parameters were used for the ultrasound pulse train as mentioned previously (8 sequential 5 ms pulses—for total duration 40 ms, peak to peak voltage 1 V, frequency 2.5 MHz). Unlike in the early diastolic set of experiments, changes in RLS were

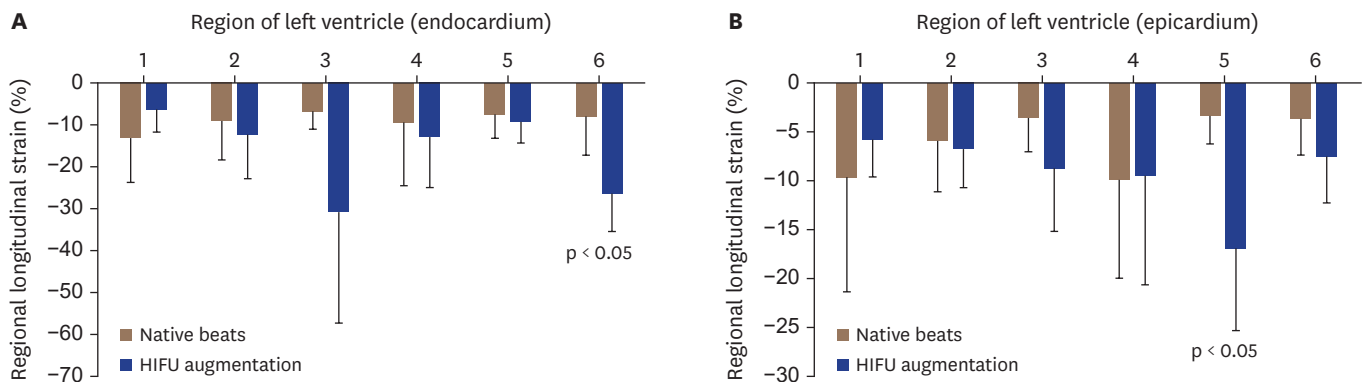


**Figure 5.** Early diastolic assessment of RLS. (A) Early diastolic RLS in the LV endocardium. The gray bars correspond to RLS measured in native beats ( $n = 5$ ). The black bars correspond to RLS measured in beats with HIFU augmentation ( $n = 5$ ). (B) Early diastolic RLS was measured in the LV epicardium for the same control and experimental animal groups.

RLS: regional longitudinal strain, LV: left ventricular, HIFU: high intensity focused ultrasound.

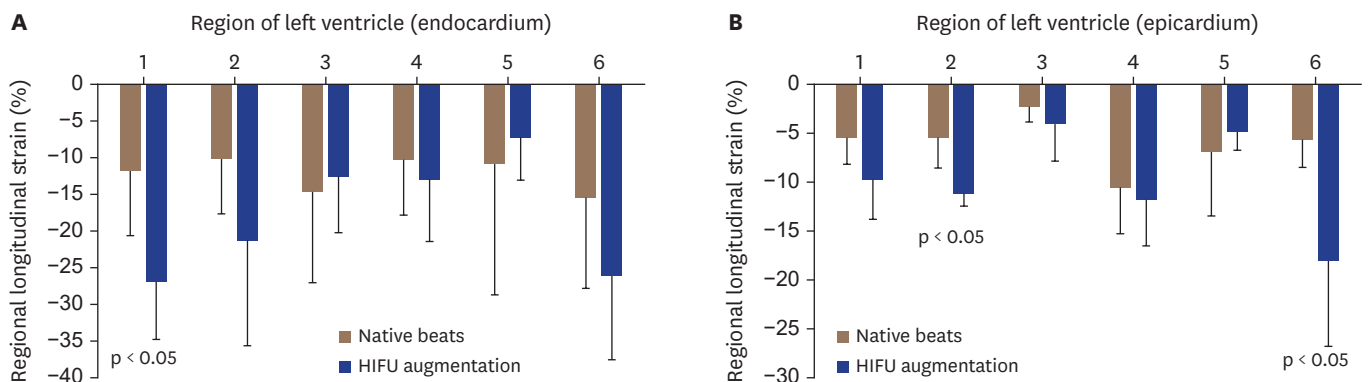


**Figure 6.** Mid diastolic assessment of RLS. (A) Mid diastolic RLS in the LV endocardium. The gray bars correspond to RLS measured in native beats ( $n = 5$ ). The black bars correspond to RLS measured in beats with HIFU augmentation ( $n = 5$ ). (B) Mid diastolic RLS was measured in the LV epicardium for the same control and experimental animal groups.

RLS: regional longitudinal strain, LV: left ventricular, HIFU: high intensity focused ultrasound.

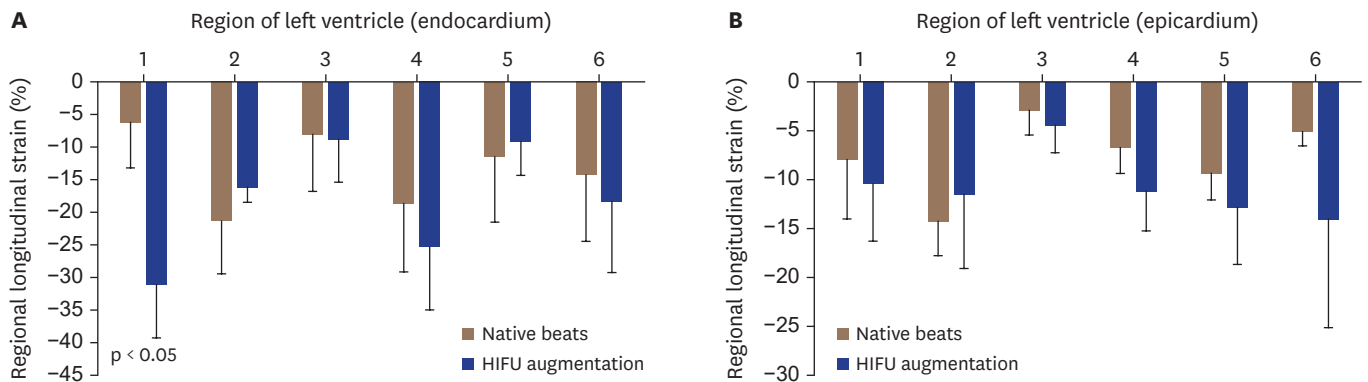


**Figure 7.** Late diastolic assessment of RLS. (A) Late diastolic RLS in the LV endocardium. The gray bars correspond to RLS measured in native beats ( $n = 5$ ). The black bars correspond to RLS measured in beats with ultrasound augmentation ( $n = 5$ ). (B) Late diastolic RLS was measured in the LV epicardium for the same control and experimental animal groups.

RLS: regional longitudinal strain, LV: left ventricular, HIFU: high intensity focused ultrasound.

noted in two non-contiguous regions of the LV. The posterior-base of the endocardium, posterior-mid region of the epicardium, as well as the anterior-apex of the epicardium experienced significant ( $p < 0.05$ ) increase in RLS with acoustic augmentation.

#### Late diastolic ultrasound augmentation

The final set of experiments targeted the anterior LV during the late diastolic time period. An offset of 130 ms was used after recognition of the R wave before deliverance of the HIFU pulse. Characteristics of the ultrasound pulse train are the same as described previously (8 sequential 5 ms pulses—for total duration 40 ms, peak to peak voltage 1 V, frequency 2.5 MHz). The results are shown in **Figure 7**. The epicardial region did not experience a statistical increase in strain with ultrasound augmentation. However, the endocardium however experienced statistically significant ( $p < 0.05$ ) increase in RLS in the posterior-base region.

## DISCUSSION

In this study, we explored a novel application of ultrasound energy to non-invasively alter regional myocardial strain in a murine model. Our experiments sought to mimic the changes seen early in the development of HF caused by ischemic CAD. By delivering a HIFU pulse over the anterior surface of the LV, we were successfully able to induce significant ( $p < 0.05$ ) changes in regional LV RLS during early, mid, and late diastole. Our use of multiple impulses in rapid succession maximized the strain induced within the myocardium, each impact creating additive changes which became significant in the regions mentioned. The specific regions within which augmentation was observed were different in each of the three time periods. This was a consequence of different areas of the LV being positioned within the path of the HIFU beam. In early diastole, significant ( $p < 0.05$ ) increase in RLS was noted in the anterior mid and apical regions which were initially within the focal point of the beam. In mid diastole, as the LV expanded, the anterior apex of the epicardium continued to show significant ( $p < 0.05$ ) RLS augmentation. However, regions of significance ( $p < 0.05$ ) spread to include the posterior mid and base regions of the epicardium and endocardium respectively as well. Finally, in late diastole, only the posterior base of the endocardium was noted to have significant ( $p < 0.05$ ) increase in RLS, because the apex was now outside the focal point of the beam. The difference between the degree of augmentation in the



endocardium and epicardium is explained by the fact that in an *in vivo* cardiac model, the heart is somewhat free to roll under the ultrasound impulse. In this setting, some of the energy is redirected to torque the heart around its tissue attachments rather than linearly travelling perpendicular through both layers. We suspect that in a fixed *ex vivo* model, the endocardium and epicardium would exhibit near identical change in strain.

By our estimation, this work is the first demonstration of ultrasound-induced augmentation of LV RLS in a small animal model. We propose that a rapid non-invasive method of inducing regional LV strain changes would be beneficial in understanding the link between ischemic CAD and the early formative stages of HFrEF and HFpEF. This application is particularly needed in the understanding of the pathogenesis of HFpEF. HFpEF constitutes a significant and growing proportion of total HF cases, with morbidity and mortality on par with HFrEF and disproportionately worsening. However, it is far more poorly understood in terms of its causative mechanisms and underlying pathophysiology.<sup>18)19)</sup> In addition, aside from diuretics for symptom management and treatment of underlying risk factors, there is a concerning lack of morbidity and mortality altering treatments available for HFpEF. This represents a very real unmet medical crisis. One culprit for the scarcity of therapies for HFpEF is the lack of representative animal experimental models that accurately simulate its early pathophysiology.<sup>20)</sup>

There are several potential areas for future work based on these results. In addition to measuring RLS, we also measured LV ejection fraction, mitral and tricuspid E/A ratios, mitral and tricuspid annular plane of systolic excursion,<sup>21-23)</sup> however we did not find significant differences in these parameters between the 2 groups. Inducing changes in these parameters will be a goal for future studies. In addition, the mouse model presents some logistical challenges. The average LV dimension in our mice was 7-10 mm in length and 5-7 mm in width. The width of the ultrasound beam was 5 mm, which is the same diameter as the aperture bored into the end of the plastic housing syringe. As the beam penetrates 3 mm of skin and connective tissue to reach the LV myocardial surface of the left ventricle, it remains in its focal zone, maintaining a stable diameter of 5 mm. The beam was aligned with the LV using anatomic landmarks,<sup>24)</sup> and positioning confirmed by the appearance of faint ultrasound interference patterns seen on echocardiography images (**Figure 3B**). However, with such a small LV area to target, it is difficult to position the ultrasound probe precisely so that the focal point is aligned directly with the center of the ventricle and remains consistently aligned throughout each delivered pulse. Even if the location of the murine LV relative to the probe tip shifts by a few millimeters (which may occur during normal respirations of the mouse), the targeting of the ultrasound pulse will no longer be optimal. The ultrasound waves could strike the edges of the ventricle, creating a torque and rolling the heart, rather than buckling it. Experimenting with larger animal models, such as a porcine model, could circumvent this issue. This would give us a larger cardiac target and more consistently allow us to strike the center of the ventricle with every pulse.

Another topic which will be addressed in future studies is the safety assessment of the delivered energy and intensity used in this manuscript. At 2.5 MHz and with acoustic output of 200 W/cm<sup>2</sup> at the mouse surface, our transducer was kept below power levels known to cause cavitation *in vivo*.<sup>25)</sup> Another area of concern is the extent of thermal effects within the myocardium. Thermal index in soft tissue, which is calculated from acoustic output and frequency,<sup>26)</sup> and the parameter around which ultrasound safety guidelines are based, does not translate well to the field of HIFU. HIFU uses short (on the order of  $\mu$ s to ms) pulses, compared to longer pulses (on the order of seconds to minutes) used in traditional diagnostic

ultrasound, for which this safety parameter was developed.<sup>27)</sup> With the very brief (5 ms per pulse, total 40 ms per pulse train) duration of our pulses, there is low risk of significant rise in temperature or damage to cardiac tissue. In comparison, HIFU pulses which have been used in literature to cause myocardial lesions have had power on the order of  $> 1,000 \text{ W/cm}^2$  and exposure time on the order of seconds.<sup>28)29)</sup> Upon dissection of the animals subjected to HIFU, inspection of the skin, rib cage, as well as the myocardial surface did not reveal any sign of edema, hemorrhage, or other damage when compared to control animals. In future large animal studies, as we utilize more powerful pulses over longer periods of time, histological analysis to look for cellular level of damage will become important.

## REFERENCES

1. D'Elia N, D'hooge J, Marwick TH. Association between myocardial mechanics and ischemic LV remodeling. *JACC Cardiovasc Imaging* 2015;8:1430-43.  
[PUBMED](#) | [CROSSREF](#)
2. Liszka J, Haberka M, Tabor Z, Finik M, Gašior Z. Two-dimensional speckle-tracking echocardiography assessment of left ventricular remodeling in patients after myocardial infarction and primary reperfusion. *Arch Med Sci* 2014;10:1091-100.  
[PUBMED](#) | [CROSSREF](#)
3. Moaref A, Zamirian M, Safari A, Emami Y. Evaluation of global and regional strain in patients with acute coronary syndrome without previous myocardial infarction. *Int Cardiovasc Res J* 2016;10:6-11.  
[CROSSREF](#)
4. Ernande L, Bergerot C, Girerd N, et al. Longitudinal myocardial strain alteration is associated with left ventricular remodeling in asymptomatic patients with type 2 diabetes mellitus. *J Am Soc Echocardiogr* 2014;27:479-88.  
[PUBMED](#) | [CROSSREF](#)
5. Tsai WC, Liu YW, Huang YY, Lin CC, Lee CH, Tsai LM. Diagnostic value of segmental longitudinal strain by automated function imaging in coronary artery disease without left ventricular dysfunction. *J Am Soc Echocardiogr* 2010;23:1183-9.  
[PUBMED](#) | [CROSSREF](#)
6. D'Andrea A, Cocchia R, Caso P, et al. Global longitudinal speckle-tracking strain is predictive of left ventricular remodeling after coronary angioplasty in patients with recent non-ST elevation myocardial infarction. *Int J Cardiol* 2011;153:185-91.  
[PUBMED](#) | [CROSSREF](#)
7. Zaliaduonyte-Peksiene D, Vaskelyte JJ, Mizariene V, Jurkevicius R, Zaliunas R. Does longitudinal strain predict left ventricular remodeling after myocardial infarction? *Echocardiography* 2012;29:419-27.  
[PUBMED](#) | [CROSSREF](#)
8. Riehle C, Bauersachs J. Small animal models of heart failure. *Cardiovasc Res* 2019;115:1838-49.  
[PUBMED](#) | [CROSSREF](#)
9. Gao E, Lei YH, Shang X, et al. A novel and efficient model of coronary artery ligation and myocardial infarction in the mouse. *Circ Res* 2010;107:1445-53.  
[PUBMED](#) | [CROSSREF](#)
10. Valero-Muñoz M, Backman W, Sam F. Murine models of heart failure with preserved ejection fraction: a "Fishing Expedition". *JACC Basic Transl Sci* 2017;2:770-89.  
[PUBMED](#) | [CROSSREF](#)
11. Torr GR. The acoustic radiation force. *Am J Phys* 1984;52:402-8.  
[CROSSREF](#)
12. Day AC, Gore DM, Bunce C, Evans JR. Laser-assisted cataract surgery versus standard ultrasound phacoemulsification cataract surgery. *Cochrane Database Syst Rev* 2016;7:CD010735.  
[PUBMED](#) | [CROSSREF](#)
13. Marquet F, Bour P, Vaillant F, et al. Non-invasive cardiac pacing with image-guided focused ultrasound. *Sci Rep* 2016;6:36534.  
[PUBMED](#) | [CROSSREF](#)
14. Bohs LN, Geiman BJ, Anderson ME, Gebhart SC, Trahey GE. Speckle tracking for multi-dimensional flow estimation. *Ultrasonics* 2000;38:369-75.  
[PUBMED](#) | [CROSSREF](#)

15. Hiesinger W, Brukman MJ, McCormick RC, et al. Myocardial tissue elastic properties determined by atomic force microscopy after stromal cell-derived factor 1 $\alpha$  angiogenic therapy for acute myocardial infarction in a murine model. *J Thorac Cardiovasc Surg* 2012;143:962-6.  
[PUBMED](#) | [CROSSREF](#)
16. Couade M, Pernot M, Messas E, et al. In vivo quantitative mapping of myocardial stiffening and transmural anisotropy during the cardiac cycle. *IEEE Trans Med Imaging* 2011;30:295-305.  
[PUBMED](#) | [CROSSREF](#)
17. IACUC guidelines and procedures. Available at: <https://drexel.edu/research/compliance/animal-care-use/guidelines-procedures/>.
18. Sharma K, Kass DA. Heart failure with preserved ejection fraction: mechanisms, clinical features, and therapies. *Circ Res* 2014;115:79-96.  
[PUBMED](#) | [CROSSREF](#)
19. Kitzman DW, Upadhy B. Heart failure with preserved ejection fraction: a heterogenous disorder with multifactorial pathophysiology. *J Am Coll Cardiol* 2014;63:457-9.  
[PUBMED](#) | [CROSSREF](#)
20. Borlaug BA. The pathophysiology of heart failure with preserved ejection fraction. *Nat Rev Cardiol* 2014;11:507-15.  
[PUBMED](#) | [CROSSREF](#)
21. Kohut A, Patel N, Singh H. Comprehensive echocardiographic assessment of the right ventricle in murine models. *J Cardiovasc Ultrasound* 2016;24:229-38.  
[PUBMED](#) | [CROSSREF](#)
22. Goswami SK, Ponnalagu D, Hussain AT, et al. Expression and activation of BK<sub>Ca</sub> channels in mice protects against ischemia-reperfusion injury of isolated hearts by modulating mitochondrial function. *Front Cardiovasc Med* 2019;5:194.  
[PUBMED](#) | [CROSSREF](#)
23. Patel NH, Johannsen J, Shah K, et al. Inhibition of BK<sub>Ca</sub> negatively alters cardiovascular function. *Physiol Rep* 2018;6:e13748 .  
[CROSSREF](#)
24. Cook MJ. The anatomy of the laboratory mouse. 1st edition. London, UK: Academic Press, 1965:89-93.
25. Hynynen K. The threshold for thermally significant cavitation in dog's thigh muscle *in vivo*. *Ultrasound Med Biol* 1991;17:157-69.  
[PUBMED](#) | [CROSSREF](#)
26. Bigelow TA, Church CC, Sandstrom K, et al. The thermal index: its strengths, weaknesses, and proposed improvements. *J Ultrasound Med* 2011;30:714-34.  
[PUBMED](#) | [CROSSREF](#)
27. Palmeri ML, Nightingale KR. On the thermal effects associated with radiation force imaging of soft tissue. *IEEE Trans Ultrason Ferroelectr Freq Control* 2004;51:551-65.  
[PUBMED](#) | [CROSSREF](#)
28. Lee LA, Simon C, Bove EL, et al. High intensity focused ultrasound effect on cardiac tissues: potential for clinical application. *Echocardiography* 2000;17:563-6.  
[PUBMED](#) | [CROSSREF](#)
29. Swaminathan A, Rieke V, King RL, Pauly J, Butts-Pauly K, McConnell M. Feasibility of noninvasive 3 T MRI-guided myocardial ablation with high intensity focused ultrasound. *J Cardiovasc Magn Reson* 2009;11 Suppl 1:O86.  
[CROSSREF](#)